Inverse dynamic modelling of a three-legged six-degree-of-freedom parallel mechanism

Sajeeva Abeywardena & Chao Chen

Multibody System Dynamics

ISSN 1384-5640

Multibody Syst Dyn
DOI 10.1007/s11044-016-9506-y

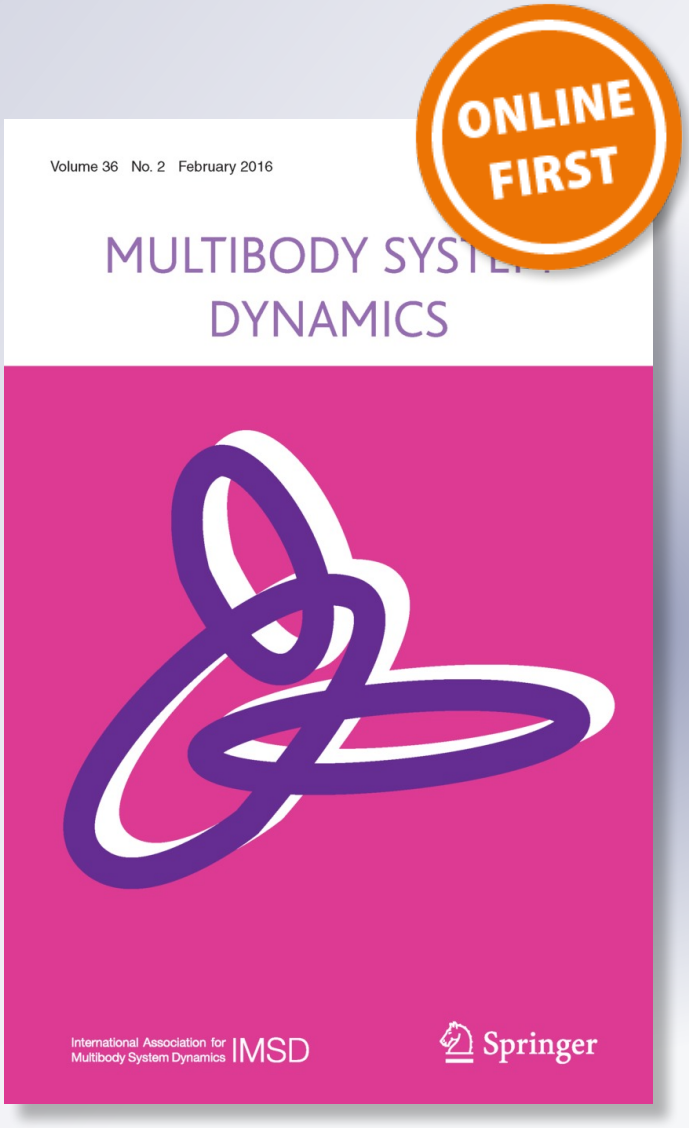

Springer

Multibody Syst Dyn
DOI 10.1007/s11044-016-9506-y

Inverse dynamic modelling of a three-legged six-degree-of-freedom parallel mechanism

Sajeeva Abeywardena[1] · **Chao Chen**[1]

Received: 23 June 2015 / Accepted: 21 January 2016

Abstract The Monash Epicyclic Parallel Manipulator (MEPaM) is a novel six-degree-of-freedom (dof) parallel mechanism with base mounted actuators. Closed form equations of the inverse dynamic model of MEPaM are obtained through two different methods, with simulation showing these models to be equivalent. The base inertial parameters for the dynamic model of MEPaM are determined, reducing the number of inertial parameters from 100 to 28. This significantly simplifies the dynamic calibration model and thus the number of computations required.

Keywords Parallel mechanisms · Inverse dynamics · Base inertial parameters

1 Introduction

The dynamics of a robotic mechanism is useful in simulation and control scenarios. Two dynamic problems exist: inverse and direct dynamics. The inverse dynamic problem determines the required actuator torques for a given trajectory of the mechanism whereas the direct dynamic problem determines the trajectory of the manipulator for a given set of actuator torques/forces. The inverse dynamic problem is associated with dynamic calibration and control of the mechanism whilst the direct dynamic problem is used in simulations [2, 7, 19].

The closed loop nature of parallel mechanisms adds significant complexity to the kinematic and dynamic models. Many techniques have been used to formulate the inverse dynamic problem of parallel mechanisms—the principle of virtual work [9, 32, 33], Kane's Equation [27], Euler–Lagrange energy based methods [14, 25] and the recursive Newton–Euler algorithm [8, 15]. The complexity of the inverse dynamic models of parallel mechanisms is increased with the introduction of constraint equations, leading to extremely large equations. However, methods exist whereby the constraint equations are naturally embedded

✉ S. Abeywardena
sajeeva.abeywardena@gmail.com

C. Chen
chao.chen@monash.edu

[1] Department of Mechanical and Aerospace Engineering, Monash University, Melbourne, Australia

Published online: 01 February 2016

into the model through the velocity constraints inherent in the mechanism, leading to closed form solutions. Khalil and Ibrahim [21] generalised methods presented in [16, 17, 20] to obtain closed form inverse dynamic models of parallel robots without the introduction of constraint equations. They consider the platform and legs as independent entities, then use the manipulator Jacobian to project the dynamics of the platform and passive joints into the active joint space. The Natural Orthogonal Complement (NOC) is another method that has been used to derive the inverse dynamics of a parallel mechanism without the use of explicit constraint equations [1, 11, 28, 31, 34, 35]. This method uses the orthogonal complement of the velocity constraint matrix (which need not be determined) to derive a closed form expression of the inverse dynamics of the mechanism in terms of only the active joint variables. Computation cost is an important factor in inverse dynamics modelling, with the NOC and Khalil–Ibrahim methods shown to be more efficient than the virtual work and Newton–Euler methods, respectively [1, 20]. However, the computational efficiency of these two methods has not been compared to date despite both methods similarly avoiding the use of explicit constraint equations.

The Monash Epicyclic Parallel Manipulator (MEPaM) is a novel three-legged six-degree-of-freedom (dof) parallel manipulator which uses a cable pulley system to allow all actuators to be mounted on the base. Three-legged six-dof parallel mechanisms with base mounted actuation have been proposed before [6, 26, 30]; however, the main focus of these works has been on design, geometric modelling and workspace analysis with scarce information on the dynamics of such mechanisms reported. It is important to investigate the dynamics of this class of manipulators as they have the least moving masses and inertias among the six-dof manipulators. Our previous study investigated the geometric models, singularities and workspace of MEPaM [5]. It was found that the mechanism has relatively simple kinematics when compared to other six-dof parallel mechanisms and interior parallel singularities which are wholly dependent on the orientation of the platform and independent of its position.

In this paper, the inverse dynamic model of MEPaM is derived using two methods—the NOC method developed by Angeles and Lee [3] and the method presented by Khalil and Ibrahim [21], with the computational efficiency of the two methods compared. Further, we derive the minimum number of inertial parameters required to calculate the inverse dynamic model of MEPaM and investigate the effect using these parameters has on the computational efficiency of the two methods. The frame assignment of MEPaM is provided in Sect. 2 and the velocity and acceleration analysis in Sect. 3. The inverse dynamic models are derived in Sect. 4, with the base inertial parameters of these models determined in Sect. 5. Finally, Sect. 6 verifies the correctness of the derived models through simulation and investigates their computational efficiency.

2 Frame assignment

MEPaM consists of three serial legs which connect to a common platform. Each leg contains a two-dof planar driving arm consisting of the planet—Lever Arm A—and the carrier—Lever Arm B—which are driven by two base-mounted rotary motors. A passive cylindrical rod which is perpendicular to the driving arm attaches to the common platform via a universal joint, forming a closed chain when all three legs are connected. A diagram of MEPaM is shown in Fig. 1.

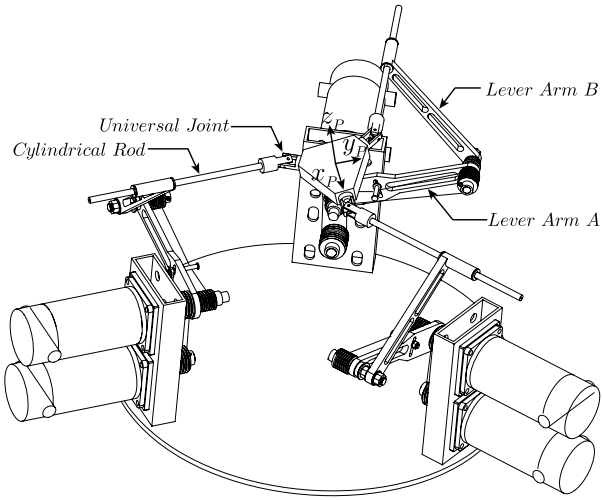

Fig. 1 The Monash Epicyclic Parallel Manipulator

Table 1 Khalil–Kleinfinger Parameters for Leg i of MEPaM ($i = 1, 2, 3$)

j	a_j	α_j	d_j	θ_j	b_j	γ_j
$1i$	w_{xi}	$\frac{\pi}{2}$	r_i	β_{ia}	w_{zi}	γ_i
$2i$	d_{1i}	0	0	β_{ib}	0	0
$3i$	d_{2i}	π	l_i	0	0	0

2.1 Serial leg frames

The frame assignment for leg i of MEPaM is shown in Fig. 2. The rotation axis of the cylindrical joint is orthogonal to the two rotation axes of the universal joint, and therefore the origin of the frame for the cylindrical joint is assigned at the universal joint origin, i.e. the connection point of the leg to the platform. Thus—to simplify the dynamic analysis—the revolute of the cylindrical joint coupled with the universal joint rotations can be considered to form a spherical joint and serve as the joint at which the serial leg is cut from the platform. Hence, the serial legs can be considered as Revolute–Revolute–Prismatic chains, with the two revolute joints being active and the prismatic joint passive. The dynamic analysis can be further simplified by assuming the links of the legs of MEPaM have 'virtual' actuators attached directly at the location of the joints. The relationship between the physical variables θ_{ia}, θ_{ib} and l_i and the 'virtual' variables β_{ia}, β_{ib} and l_i is [5]

$$\beta_{ia} = \theta_{ia}, \qquad \beta_{ib} = \theta_{ib} - \theta_{ia}, \qquad l_i = l_i. \tag{1}$$

A Jacobian relationship is used to convert the dynamic model between the two variable sets and can be written in a matrix form, i.e.

$$\dot{\boldsymbol{\theta}}_i = \mathbf{A}_\beta \dot{\boldsymbol{\beta}}_i \tag{2}$$

where $\dot{\boldsymbol{\theta}}_i = [\dot{\theta}_{ia}\ \dot{\theta}_{ib}]^T$, $\dot{\boldsymbol{\beta}}_i = [\dot{\beta}_{ia}\ \dot{\beta}_{ib}]^T$ and $\mathbf{A}_\beta = \left[\begin{smallmatrix} 1 & 0 \\ 1 & 1 \end{smallmatrix}\right]$.

The Khalil–Kleinfinger convention [22] is used to describe the geometry of the legs, with the parameters for leg i of MEPaM tabulated in Table 1.

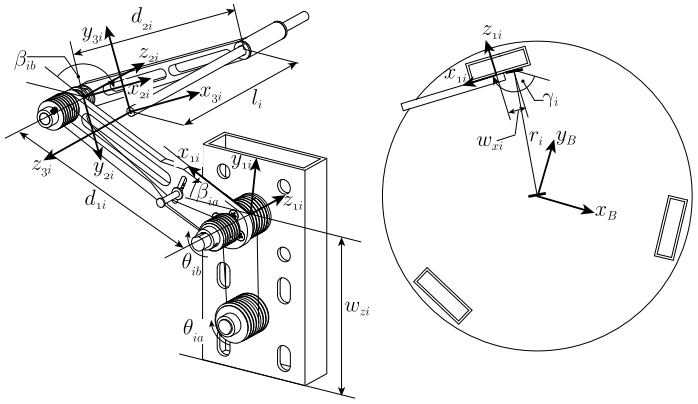

Fig. 2 Kinematic Parameters for Khalil–Kleinfinger Notation

The general transformation from the base frame $\mathcal{F}_B$ to the end effector frame $\mathcal{F}_{3i}$ for a leg of MEPaM is of form

$$ {}^{B}\mathbf{T}_{3i} = \begin{bmatrix} {}^{B}\mathbf{Q}_{3i} & {}^{B}\mathbf{p}_{3i} \\ \mathbf{0}_{1\times 3} & 1 \end{bmatrix} \tag{3} $$

where ${}^{B}\mathbf{Q}_{3i}$ is the 3×3 rotation matrix between $\mathcal{F}_B$ and $\mathcal{F}_{3i}$ and ${}^{B}\mathbf{p}_{3i}$ is the position of the end effector of the serial leg in $\mathcal{F}_B$, both in terms of the parameters in Table 1.

2.2 Platform frame

The frame assigned to the moving platform, $\mathcal{F}_P$, is used to describe the position and orientation of the platform with respect to the base frame $\mathcal{F}_B$. This relationship is described by the transformation matrix between $\mathcal{F}_B$ and $\mathcal{F}_P$, i.e.

$$ {}^{B}\mathbf{T}_{P} = \begin{bmatrix} {}^{B}\mathbf{Q}_{P} & {}^{B}\mathbf{p}_{P} \\ \mathbf{0}_{1\times 3} & 1 \end{bmatrix} \tag{4} $$

where ${}^{B}\mathbf{Q}_{P}$ is the 3×3 rotation matrix between $\mathcal{F}_B$ and $\mathcal{F}_P$ and ${}^{B}\mathbf{p}_{P}$ is the position of the platform origin in $\mathcal{F}_B$. The location of $\mathcal{F}_P$ is defined by the centre of the three universal joints of the moving platform. Figure 3 illustrates the assignment of $\mathcal{F}_P$ and the parameters of the platform. With respect to Fig. 3, the co-ordinates of the three vertices in $\mathcal{F}_P$ are

$$ {}^{P}\mathbf{b}_1 = \begin{bmatrix} d_{31} & 0 & 0 \end{bmatrix}^T, \qquad {}^{P}\mathbf{b}_2 = \begin{bmatrix} -d_{32}s_2 & d_{32}c_2 & 0 \end{bmatrix}^T, \qquad {}^{P}\mathbf{b}_3 = \begin{bmatrix} -d_{33}s_3 & -d_{33}c_3 & 0 \end{bmatrix}^T \tag{5} $$

where $c_i = \cos\psi_i$ and $s_i = \sin\psi_i$.

2.3 Position constraints

Due to the closed loop nature of MEPaM, constraints are placed onto the position of the legs and the platform. As the location of the frame origins for the serial legs are at the platform vertices—the centre of the universal joints—the position constraints are formulated

Fig. 3 Definition of $\mathcal{F}_P$

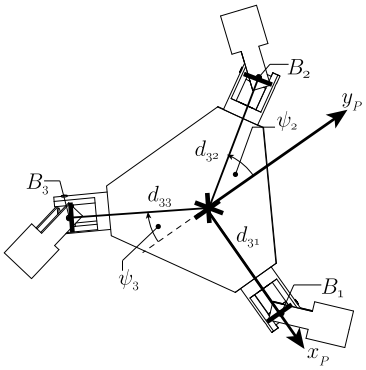

by equating the position components of Eq. (3) to the vertex co-ordinates given by Eq. (5) represented in $\mathcal{F}_B$. That is,

$$\begin{bmatrix} {}^B\mathbf{p}_{3i} \\ 1 \end{bmatrix} = {}^B\mathbf{T}_P \begin{bmatrix} {}^P\mathbf{b}_i \\ 1 \end{bmatrix}, \qquad {}^B\mathbf{p}_{3i} = {}^B\mathbf{p}_P + {}^B\mathbf{Q}_P\, {}^P\mathbf{b}_i \tag{6}$$

for $i = 1, 2, 3$. Equation (6) represents three loop equations in terms of the joint and task space variables. These loop equations are used to solve the inverse and direct geometric problems, solutions to which can be found in [5].

3 Velocity and acceleration

3.1 Twists of the serial legs

The twists (the velocity and angular velocity) of the bodies of the serial legs are derived using standard methods for serial robots which utilise the link transformation matrices defined by the parameters in Table 1, i.e. recursive algorithms outlined in robotics textbooks [2, 7, 19]. The acceleration and angular acceleration are derived similarly.

3.2 Serial leg Jacobian

The end effectors of the serial legs are expressed in terms of the active and passive joints of MEPaM. Thus, the linear velocity of the connection point to the platform—the centre of the universal joint—can be expressed in terms of the active and passive joint rates. This is given by the result of the recursive algorithm in Sect. 3.1 for link $3i$, or equivalently through differentiation of the left hand side of Eq. (6). Hence, the linear velocity of the end effector of the serial legs in the global base frame $\mathcal{F}_B$ can be expressed in the form

$${}^B\mathbf{v}_{3i} = {}^B\mathbf{J}_{3i}\dot{\mathbf{q}}_i \tag{7}$$

where ${}^B\mathbf{v}_{3i}$ is the 3×1 linear velocity vector of the end effector of leg i in $\mathcal{F}_B$, ${}^B\mathbf{J}_{3i}$ is the 3×3 serial leg Jacobian of the end effector of leg i in $\mathcal{F}_B$ and $\dot{\mathbf{q}}_i = [\dot{\beta}_{ia}\ \dot{\beta}_{ib}\ \dot{l}_i]^T$ is the vector of active and passive joint rates of leg i.

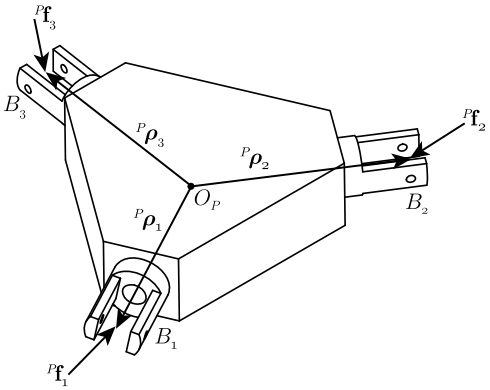

Fig. 4 Forces applied to platform by serial legs of MEPaM

3.3 Platform velocity

Considering the right hand side of Eq. (6), the linear velocity of the connection point B_i can also be expressed in terms of the twist of the platform. Letting ${}^B\boldsymbol{\rho}_i = {}^B\mathbf{Q}_P\,{}^P\mathbf{b}_i = [{}^Bb_{xi}\ {}^Bb_{yi}\ {}^Bb_{zi}]^T$ represent the vector between the origin of the platform and the platform vertices, as illustrated in Fig. 4, the linear velocity of B_i in terms of the platform twist is

$$\begin{aligned} {}^B\mathbf{v}_i &= {}^B\mathbf{v}_P + {}^B\boldsymbol{\omega}_P \times {}^B\boldsymbol{\rho}_i \\ &= \begin{bmatrix} \mathbf{1}_3 & -{}^B\hat{\boldsymbol{\rho}}_i \end{bmatrix} \begin{bmatrix} {}^B\mathbf{v}_P \\ {}^B\boldsymbol{\omega}_P \end{bmatrix} \\ &= {}^B\mathbf{J}_{ti}\,{}^B\mathbf{t}_P \end{aligned} \tag{8}$$

where ${}^B\hat{\boldsymbol{\rho}}_i$ is the skew-symmetric matrix associated with ${}^B\boldsymbol{\rho}_i$ which performs the cross-product, ${}^B\mathbf{t}_P$ is the twist of the platform with respect to the base frame and ${}^B\mathbf{J}_{ti}$ is the platform Jacobian with respect to the base frame for point B_i.

3.4 Manipulator Jacobian

Due to the position constraints given by Eq. (6), Eqs. (7) and (8) are equivalent and represent the velocity constraints of MEPaM, i.e.

$${}^B\mathbf{J}_{3i}\dot{\mathbf{q}}_i = {}^B\mathbf{J}_{ti}\,{}^B\mathbf{t}_P. \tag{9}$$

As a result of Eq. (9), the joint rates of leg i can be written in terms of the twist of the platform,

$$\dot{\mathbf{q}}_i = {}^B\mathbf{J}_{3i}^{-1}\,{}^B\mathbf{J}_{ti}\,{}^B\mathbf{t}_P. \tag{10}$$

Concatenating Eq. (10) for $i = 1, 2, 3$ yields

$$\begin{aligned} \begin{bmatrix} \dot{\mathbf{q}}_1 \\ \dot{\mathbf{q}}_2 \\ \dot{\mathbf{q}}_3 \end{bmatrix} &= \begin{bmatrix} {}^B\mathbf{J}_{31}^{-1}\,{}^B\mathbf{J}_{t1} \\ {}^B\mathbf{J}_{32}^{-1}\,{}^B\mathbf{J}_{t2} \\ {}^B\mathbf{J}_{33}^{-1}\,{}^B\mathbf{J}_{t3} \end{bmatrix} {}^B\mathbf{t}_P, \\ \dot{\mathbf{q}} &= {}^B\mathbf{J}_F^{-1}\,{}^B\mathbf{t}_P \end{aligned} \tag{11}$$

where ${}^{B}\mathbf{J}_{F}^{-1}$ is a 9×6 matrix which relates all the joint rates of MEPaM—active and passive—to the twist of the platform. This matrix can be simplified by only considering the active joints, i.e.

$$\begin{bmatrix} \dot{\mathbf{q}}_{A1} \\ \dot{\mathbf{q}}_{A2} \\ \dot{\mathbf{q}}_{A3} \end{bmatrix} = \begin{bmatrix} {}^{B}\mathbf{J}_{31}^{-1}(1:2,:){}^{B}\mathbf{J}_{t1} \\ {}^{B}\mathbf{J}_{32}^{-1}(1:2,:){}^{B}\mathbf{J}_{t2} \\ {}^{B}\mathbf{J}_{33}^{-1}(1:2,:){}^{B}\mathbf{J}_{t3} \end{bmatrix} {}^{B}\mathbf{t}_{P}, \qquad \dot{\mathbf{q}}_{A} = {}^{B}\mathbf{J}_{M}^{-1}{}^{B}\mathbf{t}_{P} \tag{12}$$

where ${}^{B}\mathbf{J}_{M}$ is the 6×6 manipulator Jacobian relating the twist of the platform to the rates of the active joints $\dot{\mathbf{q}}_{A}$. Note that ${}^{B}\mathbf{J}_{3i}^{-1}(1:2,:)$ indicates that only row 1 and 2 of the inverse serial Jacobian matrix of interest is considered as these correspond to the active joint variables β_{ia} and β_{ib}. Further, the manipulator Jacobian expressed in $\mathcal{F}_{P}$ is

$${}^{P}\mathbf{J}_{M} = \begin{bmatrix} {}^{B}\mathbf{Q}_{P}^{T} & \mathbf{0}_{3\times3} \\ \mathbf{0}_{3\times3} & {}^{B}\mathbf{Q}_{P}^{T} \end{bmatrix} {}^{B}\mathbf{J}_{M}. \tag{13}$$

The linear and angular acceleration of the platform can then be found by differentiating Eq. (12), i.e.

$${}^{B}\dot{\mathbf{t}}_{P} = {}^{B}\mathbf{J}_{M}\ddot{\mathbf{q}}_{A} + {}^{B}\dot{\mathbf{J}}_{M}\dot{\mathbf{q}}_{A}. \tag{14}$$

Equation (14) are the acceleration constraints of the manipulator.

3.5 Passive joint rates

The dynamic model requires the rates of change of the passive joints. Considering that these correspond to the three rows of ${}^{B}\mathbf{J}_{F}^{-1}$ given by Eq. (11) ignored in Eq. (12), they can be expressed in terms of the twist of the platform as

$$\begin{bmatrix} \dot{l}_1 \\ \dot{l}_2 \\ \dot{l}_3 \end{bmatrix} = \begin{bmatrix} {}^{B}\mathbf{J}_{31}^{-1}(3,:){}^{B}\mathbf{J}_{t1} \\ {}^{B}\mathbf{J}_{32}^{-1}(3,:){}^{B}\mathbf{J}_{t2} \\ {}^{B}\mathbf{J}_{33}^{-1}(3,:){}^{B}\mathbf{J}_{t3} \end{bmatrix} {}^{B}\mathbf{t}_{P}, \qquad \dot{\mathbf{l}} = \mathbf{J}_{L}{}^{B}\mathbf{t}_{P}. \tag{15}$$

Further, through substitution of Eq. (12) into Eq. (15) for the twist of the platform, the rates of the passive joints can be expressed in terms of the rates of the active joints, i.e.

$$\dot{\mathbf{l}} = \mathbf{J}_{L}{}^{B}\mathbf{J}_{M}\dot{\mathbf{q}}_{A}. \tag{16}$$

Thus, the acceleration of the passive joints can be found in terms of the active joints, i.e.

$$\ddot{\mathbf{l}} = \mathbf{J}_{L}{}^{B}\mathbf{J}_{M}\ddot{\mathbf{q}}_{A} + \dot{\mathbf{J}}_{L}{}^{B}\mathbf{J}_{M}\dot{\mathbf{q}}_{A} + \mathbf{J}_{L}{}^{B}\dot{\mathbf{J}}_{M}\dot{\mathbf{q}}_{A}. \tag{17}$$

4 Inverse dynamic modelling

The inverse dynamic model of a parallel mechanism calculates the required torques to achieve a specified trajectory; typically as a function of the position, velocity and acceleration of the joint variables of the legs and the Cartesian coordinates of the platform of the

manipulator. The inverse dynamic model of MEPaM is formulated using two methods—the Natural Orthogonal Complement and the method of Khalil and Ibrahim [21]. Both these methods embed the constraints imposed by the closed-loop nature of the mechanism into the modelling procedure via the velocity relationships derived in Sect. 3. This avoids the use of explicit constraint equations and allows for closed form solutions to be obtained. Frictional effects are not considered in the derivation of the models.

4.1 Natural orthogonal complement

4.1.1 Overview

The Natural Orthogonal Complement (NOC) was originally used to solve the inverse dynamics of serial mechanisms [3, 4] and later parallel mechanisms [1, 11, 28, 31, 34, 35]. These mechanisms consist of p rigid bodies under holonomic constraints. The NOC method uses the wrench of each of the bodies in its derivation of the inverse dynamic model, whereby the wrench ${}^i\mathbf{w}_i$ is given by the Newton–Euler equation. For the ith body in frame $\mathcal{F}_i$, the Newton–Euler equation at the origin of $\mathcal{F}_i$ can be written as [19]

$$ {}^i\mathbf{w}_i = \begin{bmatrix} m_i\mathbf{1}_3 & -{}^i\hat{\boldsymbol{\eta}}_i \\ {}^i\hat{\boldsymbol{\eta}}_i & {}^i\mathbf{I}_i \end{bmatrix} \begin{bmatrix} {}^i\dot{\mathbf{v}}_i - {}^i\mathbf{g} \\ {}^i\dot{\boldsymbol{\omega}}_i \end{bmatrix} + \begin{bmatrix} {}^i\boldsymbol{\omega}_i \times ({}^i\boldsymbol{\omega}_i \times {}^i\boldsymbol{\eta}_i) \\ {}^i\boldsymbol{\omega}_i \times ({}^i\mathbf{I}_i{}^i\boldsymbol{\omega}_i) \end{bmatrix} \tag{18} $$

where

- ${}^i\mathbf{w}_i = [{}^i\mathbf{f}_i{}^T \ {}^i\mathbf{n}_i^T]^T$ is the wrench of the ith body acting at the origin of $\mathcal{F}_i$;
- ${}^i\mathbf{v}_i$ and ${}^i\boldsymbol{\omega}_i$ are the linear and angular velocities of the ith body with ${}^i\dot{\mathbf{v}}_i$ and ${}^i\dot{\boldsymbol{\omega}}_i$ the associated linear and angular accelerations in $\mathcal{F}_i$;
- ${}^i\mathbf{g}$ is the 3×1 vector of the acceleration due to gravity in $\mathcal{F}_i$;
- m_i is the mass of the ith body;
- ${}^i\mathbf{I}_i$ is the 3×3 inertia matrix of the ith body in $\mathcal{F}_i$, with ${}^i\mathbf{I}_i = \begin{bmatrix} XX_i & XY_i & XZ_i \\ XY_i & YY_i & YZ_i \\ XZ_i & YZ_i & ZZ_i \end{bmatrix}$;
- ${}^i\boldsymbol{\eta}_i = m_i{}^i\mathbf{s}_i = [MX_i, MY_i, MZ_i]^T$ are the first moments around the origin of $\mathcal{F}_i$ with ${}^i\hat{\boldsymbol{\eta}}_i$ being the associated skew-symmetric matrix;
- ${}^i\mathbf{s}_i$ is the 3×1 vector from the origin of $\mathcal{F}_i$ to the centre of mass of the ith body; and
- $\mathbf{1}_3$ is the 3×3 identity matrix.

Through the use of the properties of vector cross products, Eq. (18) can be expressed as

$$ \begin{aligned} {}^i\mathbf{w}_i &= \begin{bmatrix} m_i\mathbf{1}_3 & -{}^i\hat{\boldsymbol{\eta}}_i \\ {}^i\hat{\boldsymbol{\eta}}_i & {}^i\mathbf{I}_i \end{bmatrix} {}^i\dot{\mathbf{t}}_i + \begin{bmatrix} \mathbf{0}_{3\times3} & -{}^i\hat{\boldsymbol{\omega}}_i{}^i\hat{\boldsymbol{\eta}}_i \\ \mathbf{0}_{3\times3} & {}^i\hat{\boldsymbol{\omega}}_i{}^i\mathbf{I}_i \end{bmatrix} {}^i\mathbf{t}_i - \begin{bmatrix} m_i\mathbf{1}_3 \\ {}^i\hat{\boldsymbol{\eta}}_i \end{bmatrix} {}^i\mathbf{g} \\ &= \mathbf{M}_i{}^i\dot{\mathbf{t}}_i + \mathbf{W}_i{}^i\mathbf{t}_i - \mathbf{G}_i{}^i\mathbf{g} \end{aligned} \tag{19} $$

where ${}^i\mathbf{t}_i = [{}^i\mathbf{v}_i{}^T \ {}^i\boldsymbol{\omega}_i^T]^T$ is the twist of the ith body and ${}^i\hat{\boldsymbol{\omega}}_i$ is the skew-symmetric matrix associated with ${}^i\boldsymbol{\omega}_i$.

The wrench, ${}^i\mathbf{w}_i$, can be decomposed into a working (${}^i\mathbf{w}_i^W$) and non-working (${}^i\mathbf{w}_i^N$) wrench. The working wrench can be further decomposed to consist of actuator (${}^i\mathbf{w}_i^a$), dissipate (${}^i\mathbf{w}_i^d$) and gravity (${}^i\mathbf{w}_i^g$) wrenches, i.e. ${}^i\mathbf{w}_i^W = {}^i\mathbf{w}_i^a + {}^i\mathbf{w}_i^d + {}^i\mathbf{w}_i^g$ [3, 4]. Note that ${}^i\mathbf{w}_i^g$ has been accounted for in Eq. (19). Thus, applying Eq. (19) to all p bodies, a system of equations can be derived, i.e.

$$ \mathbf{w}^W + \mathbf{w}^N = \mathbf{M}\dot{\mathbf{t}} + \mathbf{W}\mathbf{t} - \mathbf{G}\mathbf{g} \tag{20} $$

where

- $\mathbf{M} = \text{diag}([\mathbf{M}_1 \dots \mathbf{M}_p])$ and $\mathbf{W} = \text{diag}([\mathbf{W}_1 \dots \mathbf{W}_p])$ are $6p \times 6p$ generalised matrices;
- $\mathbf{G} = \text{diag}([\mathbf{G}_1 \dots \mathbf{G}_p])$ is a $6p \times 3p$ matrix;
- $\mathbf{t} = [{}^1\mathbf{t}_1^T \ \dots \ {}^p\mathbf{t}_p^T]^T$, $\mathbf{w}^W = [{}^1\mathbf{w}_1^{W\,T} \ \dots \ {}^p\mathbf{w}_p^{W\,T}]^T$ and $\mathbf{w}^N = [{}^1\mathbf{w}_1^{N\,T} \ \dots \ {}^p\mathbf{w}_p^{N\,T}]^T$ are $6p$ dimensional vectors; and
- $\mathbf{g} = [{}^1\mathbf{g}_1^T \ \dots \ {}^p\mathbf{g}_p^T]^T$ is a $3p$ dimensional vector.

It was shown that the kinematic constraints of a mechanism under holonomic constraints obeys the following relationship with $\mathbf{t}$ [3, 4],

$$\mathbf{K}\mathbf{t} = \mathbf{0}_{6p} \tag{21}$$

where $\mathbf{K}$ is the $6p \times 6p$ velocity constraint matrix of rank m—the number of independent holonomic constraints—whilst the number of degrees-of-freedom is $n = 6p - m$. This means that the generalised twist $\mathbf{t}$ can be written in terms of the independent variables $\boldsymbol{\alpha}$, i.e.

$$\mathbf{t} = \mathbf{S}\dot{\boldsymbol{\alpha}}, \qquad \dot{\mathbf{t}} = \mathbf{S}\ddot{\boldsymbol{\alpha}} + \dot{\mathbf{S}}\dot{\boldsymbol{\alpha}} \tag{22}$$

where $\mathbf{S}$ is the twist mapping matrix of dimension $6p \times n$.

Substituting Eq. (22) into Eq. (21) yields

$$\mathbf{K}\mathbf{S} = \mathbf{0}_{6p}. \tag{23}$$

Hence, $\mathbf{S}$ is the natural orthogonal complement of $\mathbf{K}$. It was shown that the non-working wrench lies in the null-space of $\mathbf{S}^T$, thus pre-multiplication of Eq. (20) eliminates $\mathbf{w}^N$ [3, 4], i.e.

$$\mathbf{S}^T\mathbf{w}^a = \mathbf{S}^T\mathbf{M}\dot{\mathbf{t}} + \mathbf{S}^T\mathbf{W}\mathbf{t} - \mathbf{S}^T\mathbf{G}\mathbf{g} - \mathbf{S}^T\mathbf{w}^d. \tag{24}$$

Substitution of Eq. (22) into Eq. (24) for $\mathbf{t}$ and $\dot{\mathbf{t}}$ results in

$$\boldsymbol{\tau}^a = \mathbf{I}\ddot{\boldsymbol{\alpha}} + \mathbf{C}\dot{\boldsymbol{\alpha}} - \boldsymbol{\tau}^g - \boldsymbol{\tau}^d \tag{25}$$

where $\mathbf{I} = \mathbf{S}^T\mathbf{M}\mathbf{S}$ is the $n \times n$ generalised inertia matrix, $\mathbf{C} = \mathbf{S}^T(\mathbf{M}\dot{\mathbf{S}} + \mathbf{W}\mathbf{S})$ is the $n \times n$ generalised coupling matrix and $\boldsymbol{\tau}^g = \mathbf{S}^T\mathbf{G}\mathbf{g}$, $\boldsymbol{\tau}^d = \mathbf{S}^T\mathbf{w}^d$, $\boldsymbol{\tau}^a = \mathbf{S}^T\mathbf{w}^a$ are the $n \times 1$ vectors of generalised gravity, dissipate and actuator forces, respectively [3, 4]. Hence, Eq. (25) represents the inverse dynamic model of the mechanism of interest obtained through the NOC method. Further, the inverse dynamic model derived using the NOC method is wholly in terms of the rates of the independent variables $\boldsymbol{\alpha}$.

4.1.2 NOC and MEPaM

To derive the inverse dynamic model of MEPaM using the NOC method, the wrenches and twists of all the bodies of MEPaM need to be derived. MEPaM consists of ten rigid bodies—three for each of the legs plus the platform. The wrenches of the bodies are given by Eq. (19), with the twists of the legs derived using standard methods for serial robots, i.e. recursive algorithms outlined in robotics textbooks [2, 7, 19]. As a result, the twist of body ji (i.e. the jth body of the ith leg of MEPaM) in $\mathcal{F}_{ji}$ can be written as

$${}^{ji}\mathbf{t}_{ji} = {}^{ji}\mathbf{Y}_{ji}\dot{\mathbf{q}} \tag{26}$$

where ${}^{ji}\mathbf{Y}_{ji}$ is a 6×9 Jacobian matrix relating the twist of body ji to the rates of all the joints of MEPaM. However, the NOC method requires the twists of the bodies to be expressed in terms of only the active joint rates $\dot{\mathbf{q}}_A$. From Eq. (16), the passive joint rates are expressed with respect to the active joint rates, thus Eq. (26) can be written as

$$ {}^{ji}\mathbf{t}_{ji} = {}^{ji}\mathbf{S}_{ji}\dot{\mathbf{q}}_A \tag{27} $$

where ${}^{ji}\mathbf{S}_{ji}$ is a 6×6 Jacobian (twist mapping) matrix relating the twist of body ji to the active joint rates of MEPaM. Further, the twist of the platform ${}^{P}\mathbf{t}_P$ in $\mathcal{F}_P$ can be written in terms of the active joint rates using Eq. (13), i.e.

$$ {}^{P}\mathbf{t}_P = {}^{P}\mathbf{J}_M\dot{\mathbf{q}}_A. \tag{28} $$

Thus the twists of all the bodies of MEPaM are known in terms of the active joint rates. Hence, the generalised twist of MEPaM is of form

$$ \begin{bmatrix} {}^{11}\mathbf{t}_{11} \\ {}^{21}\mathbf{t}_{21} \\ {}^{31}\mathbf{t}_{31} \\ {}^{12}\mathbf{t}_{12} \\ {}^{22}\mathbf{t}_{22} \\ {}^{32}\mathbf{t}_{32} \\ {}^{13}\mathbf{t}_{13} \\ {}^{23}\mathbf{t}_{23} \\ {}^{33}\mathbf{t}_{33} \\ {}^{P}\mathbf{t}_P \end{bmatrix} = \begin{bmatrix} {}^{11}\mathbf{S}_{11} \\ {}^{21}\mathbf{S}_{21} \\ {}^{31}\mathbf{S}_{31} \\ {}^{12}\mathbf{S}_{12} \\ {}^{22}\mathbf{S}_{22} \\ {}^{32}\mathbf{S}_{32} \\ {}^{13}\mathbf{S}_{13} \\ {}^{23}\mathbf{S}_{23} \\ {}^{33}\mathbf{S}_{33} \\ {}^{P}\mathbf{J}_M \end{bmatrix} \begin{bmatrix} \dot{\beta}_{1a} \\ \dot{\beta}_{1b} \\ \dot{\beta}_{2a} \\ \dot{\beta}_{2b} \\ \dot{\beta}_{3a} \\ \dot{\beta}_{3b} \end{bmatrix}, \tag{29} $$

$$ \mathbf{t}_M = \mathbf{S}_M\dot{\mathbf{q}}_A $$

where $\mathbf{t}_M$ is the 60×1 generalised twist vector of MEPaM and $\mathbf{S}_M$ is the 60×60 twist mapping matrix of MEPaM.

With the twist mapping matrix known, the inverse dynamic model of MEPaM in terms of the $\boldsymbol{\beta}$ variables, $\boldsymbol{\lambda}$, can be derived using Eq. (25), i.e.

$$ \boldsymbol{\lambda} = \mathbf{I}_M\ddot{\mathbf{q}}_A + \mathbf{C}_M\dot{\mathbf{q}}_A - \boldsymbol{\lambda}^g \tag{30} $$

where $\mathbf{I}_M$ is the 6×6 generalised inertia matrix of MEPaM, $\mathbf{C}_M$ is the 6×6 generalised coupling matrix and $\boldsymbol{\lambda}^g$ is the 6×1 vector of generalised gravity forces.

4.2 Khalil–Ibrahim method

The Khalil–Ibrahim method cuts the legs from the platform at the connection joint (i.e. the S-joint for analysis of MEPaM), with the dynamics of the legs and platform derived as independent entities. The Jacobians in Sect. 3 are used to link the subsystems together, with the dynamics of the platform and passive joints projected into the active joint space through ${}^{B}\mathbf{J}_M$, such that the inverse dynamic model is given by

$$ \boldsymbol{\lambda} = \mathbf{h}^a + {}^{B}\mathbf{J}_M^T\left({}^{B}\mathbf{w}_P + \sum_{i=1}^{m} {}^{B}\mathbf{J}_{ti}^T\,{}^{B}\mathbf{J}_i^{-T}(:, \mathbf{c}_i)\mathbf{h}_i^p\right) \tag{31} $$

where $\boldsymbol{\lambda}$ is the vector of actuator torques, ${}^{B}\mathbf{w}_{P}$ is the wrench of the platform in $\mathcal{F}_B$, $\mathbf{h_i}$ is the inverse dynamic model of the ith leg with $\mathbf{h}^{a}$ being the vector of active joint torques, $\mathbf{h}^{p}$ the vector of passive joint torques and $\mathbf{c}_i$ are the columns associated with the passive joints. In the proceeding subsections, it is shown how Eq. (31) is obtained through the derivation of the inverse dynamic model of MEPaM.

4.2.1 Platform and leg dynamics

The wrench of the platform of MEPaM is described by the Newton–Euler equation, i.e. Eq. (19), with the reference point chosen to be the origin of $\mathcal{F}_P$. Note that as this wrench is with respect to $\mathcal{F}_B$, the first moment of the platform is ${}^{B}\boldsymbol{\eta}_{P} = {}^{B}\mathbf{Q}_{P}\,{}^{P}\boldsymbol{\eta}_{P}$ and the inertia tensor is ${}^{B}\mathbf{I}_{P} = {}^{B}\mathbf{Q}_{P}\,{}^{P}\mathbf{I}_{P}\,{}^{B}\mathbf{Q}_{P}^{T}$.

The inverse dynamic model of the legs of MEPaM can be derived using classical techniques for serial robots such as the Euler–Lagrange, recursive Newton–Euler or NOC methods found in robotics textbooks, i.e. [2, 7, 19]. These methods will yield the same symbolic closed form expression for the inverse dynamics of the serial legs which are used in formulating the complete inverse dynamic model of MEPaM.

4.2.2 Motor torques

The motor torques in terms of the β variables, $\boldsymbol{\lambda}$, are determined by combining the dynamic models of the platform and the legs. The wrench of the platform ${}^{B}\mathbf{w}_{P}$ consists of the force, ${}^{B}\mathbf{f}_{P}$, and torque, ${}^{B}\boldsymbol{\tau}_{P}$, that the platform exerts onto an external environment. This force and torque is generated by the forces and torques applied to the platform by the serial legs of MEPaM. Due to the assumption of considering the connection joint of the legs to the platform to be a spherical joint, the torque applied by the legs on the platform is zero, i.e. ${}^{B}\boldsymbol{\tau}_{i} = \mathbf{0}$. Thus, the legs only produce a three dimensional force, ${}^{B}\mathbf{f}_{i}$, on the platform. With aid of Fig. 4, the wrench of the platform can be derived as

$$ {}^{B}\mathbf{w}_{P} = \begin{bmatrix} {}^{B}\mathbf{f}_{P} \\ {}^{B}\boldsymbol{\tau}_{P} \end{bmatrix} = \sum_{i=1}^{3} \begin{bmatrix} \mathbf{1}_{3} \\ {}^{B}\hat{\boldsymbol{\rho}}_{i} \end{bmatrix} {}^{B}\mathbf{f}_{i}. \tag{32} $$

Due to the properties of skew-symmetric matrices, ${}^{B}\hat{\boldsymbol{\rho}}_{i} = -{}^{B}\hat{\boldsymbol{\rho}}_{i}^{T}$. Hence, with reference to Eq. (8), Eq. (32) becomes

$$ {}^{B}\mathbf{w}_{P} = \sum_{i=1}^{3} {}^{B}\mathbf{J}_{ti}^{T}\,{}^{B}\mathbf{f}_{i}. \tag{33} $$

Thus, the task at hand is to find the forces, ${}^{B}\mathbf{f}_{i}$, that the legs exert on the platform.

The motor torques for the individual legs can be written in terms of the dynamic model, i.e.

$$ \boldsymbol{\lambda}_{i} = \mathbf{h}_{i} + {}^{B}\mathbf{J}_{3i}^{T}\,{}^{B}\mathbf{f}_{i} \tag{34} $$

where $\mathbf{h}_i$ is the inverse dynamic model of the serial leg i, ${}^{B}\mathbf{f}_{i}$ is the reaction force between the serial leg and platform which is mapped into the joint space of the leg through the transpose of the serial leg Jacobian ${}^{B}\mathbf{J}_{3i}$ and $\boldsymbol{\lambda_i}$ is the vector of motor torques for leg i. As the third joint of leg i is a passive prismatic joint, the corresponding motor torque is 0. Hence, the motor torque of leg i is

$$ \boldsymbol{\lambda}_{i} = \begin{bmatrix} \lambda_{ia} & \lambda_{ib} & 0 \end{bmatrix}^{T} \tag{35} $$

with λ_{ia} being the torque for the virtual motor associated with the variable β_{ia} and λ_{ib} the torque for the virtual motor associated with the variable β_{ib}.

Equation (34) can be rearranged to express the reaction force in terms of the motor torques and leg dynamic model, i.e.

$$^{B}\mathbf{f}_i = {}^{B}\mathbf{J}_{3i}^{-T}(\boldsymbol{\lambda}_i - \mathbf{h}_i). \tag{36}$$

Substituting Eq. (36) into Eq. (33) for $^{B}\mathbf{f}_i$ yields

$$\begin{aligned} {}^{B}\mathbf{w}_P &= \sum_{i=1}^{3} {}^{B}\mathbf{J}_{ti}^{T}\,{}^{B}\mathbf{J}_{3i}^{-T}(\boldsymbol{\lambda}_i - \mathbf{h}_i), \\ \sum_{i=1}^{3} {}^{B}\mathbf{J}_{ti}^{T}\,{}^{B}\mathbf{J}_{3i}^{-T}\boldsymbol{\lambda}_i &= {}^{B}\mathbf{w}_P + \sum_{i=1}^{3} {}^{B}\mathbf{J}_{ti}^{T}\,{}^{B}\mathbf{J}_{3i}^{-T}\mathbf{h}_i. \end{aligned} \tag{37}$$

Using Eqs. (11), (12) and (35), Eq. (37) becomes

$$\begin{aligned} \sum_{i=1}^{3} {}^{B}\mathbf{J}_{ti}^{T}\,{}^{B}\mathbf{J}_{3i}^{-T}(:,1:2)\begin{bmatrix}\lambda_{ia}\\ \lambda_{ib}\end{bmatrix} &= {}^{B}\mathbf{w}_P + \sum_{i=1}^{3} {}^{B}\mathbf{J}_{ti}^{T}\,{}^{B}\mathbf{J}_{3i}^{-T}\mathbf{h}_i \\ {}^{B}\mathbf{J}_{M}^{-T}\begin{bmatrix}\boldsymbol{\lambda}_{A1}\\ \boldsymbol{\lambda}_{A2}\\ \boldsymbol{\lambda}_{A3}\end{bmatrix} &= {}^{B}\mathbf{w}_P + {}^{B}\mathbf{J}_{F}^{-T}\begin{bmatrix}\mathbf{h}_1\\ \mathbf{h}_2\\ \mathbf{h}_3\end{bmatrix} \end{aligned} \tag{38}$$

where $\boldsymbol{\lambda}_{Ai} = [\lambda_{ia}\ \lambda_{ib}]^T$ and $\mathbf{h}_i = [h_{1i}\ h_{2i}\ h_{3i}]^T$.

Thus, the motor torques for MEPaM in terms of the dynamics of the legs and platform is

$$\boldsymbol{\lambda} = {}^{B}\mathbf{J}_{M}^{T}\left({}^{B}\mathbf{w}_P + {}^{B}\mathbf{J}_{F}^{-T}\mathbf{h}\right) \tag{39}$$

where $\boldsymbol{\lambda} = [\boldsymbol{\lambda}_{A1}^T\ \boldsymbol{\lambda}_{A2}^T\ \boldsymbol{\lambda}_{A3}^T]^T$.

The Jacobian transpose maps a Cartesian force into the active joint space of the robot, hence the terms of $\mathbf{h}_i$ corresponding to the active joints of MEPaM can be extracted out of the bracketed term of Eq. (39), i.e. the columns for which $^{B}\mathbf{J}_{M}^{T}\,{}^{B}\mathbf{J}_{F}^{-T}$ contains one entry which is 1 and the other five are 0. Thus, the inverse dynamic equation of MEPaM in terms of the β-variables is

$$\boldsymbol{\lambda} = \mathbf{h}^a + {}^{B}\mathbf{J}_{M}^{T}\left({}^{B}\mathbf{w}_P + \sum_{i=1}^{3} {}^{B}\mathbf{J}_{ti}^{T}\,{}^{B}\mathbf{J}_{3i}^{-T}(:,3)\mathbf{h}_i^p\right) \tag{40}$$

where $\mathbf{h}^a = [h_{11}\ h_{21}\ h_{12}\ h_{22}\ h_{13}\ h_{23}]^T$ correspond to the inverse dynamic model of the active revolute joint and $\mathbf{h}^p = [h_{31}\ h_{32}\ h_{33}]^T$ are the inverse dynamic models of the passive joints.

4.3 Inverse dynamic model for the actual motors

The models of Eqs. (30) and (40) do not account for the base mounted actuation of the legs of MEPaM, they are derived assuming that the actuators are directly mounted at the joints. The torques required for the actual system, $\boldsymbol{\tau}_i$, can be obtained by using the Jacobian relationship given by Eq. (2) i.e.

$$\boldsymbol{\tau} = \mathbf{J}_{\beta}^{T}\boldsymbol{\lambda} \tag{41}$$

where $\mathbf{J}_\beta^T = \text{diag}([\mathbf{A}_\beta^T\ \mathbf{A}_\beta^T\ \mathbf{A}_\beta^T])$ is a 6×6 mapping matrix. Hence, the inverse dynamic model of MEPaM has been found.

4.4 Comparison

The NOC and Khalil–Ibrahim methods both obtain closed form expressions of the inverse dynamic model of MEPaM. With regards to computation, the NOC method will require more operations due to the presence of large matrices. This inference is explored in Sect. 6. Through expressing the twists of all the rigid bodies in terms of the active joint rates, the NOC method produces a model that is completely in terms of the active joints whilst the Khalil–Ibrahim method can be made to do so through substitution of Eqs. (12) and (14) for the platform rates and Eqs. (16)–(17) for the passive joint rates.

Expressing the model in terms of only the active variables is advantageous in most instances but there are situations when this may not be the case. Dynamic calibration utilises the inverse dynamic model to identify the inertial parameters of a mechanism, with accurate knowledge of these parameters paramount in dynamically compensated control algorithms. A trajectory is prescribed and implemented for the mechanism to follow, with measurements of the active joints position (i.e. by an encoder) and the torques of the motors (i.e. a motor current) made in this situation. As the inverse dynamic model can be expressed in a linear form with respect to the inertial parameters [19, 24], the inertial parameters are found by solving an over-determined linear system of equations whereby the coefficient matrix is populated in terms of the geometric parameters and the position, velocities and accelerations of the joint and task space variables. Typically, the passive joint and task space variables are expressed in terms of the active variables, i.e. the passive joint rates are given by Eqs. (16)–(17) and task space rates given by Eqs. (12) and (14). However, if there are redundant sensors measuring the passive joints or an inertial measurement unit on the platform, the rates of the passive joints and/or the platform can be measured as opposed to estimated. This can improve the accuracy of the inertial parameter estimation and hence the computed torque calculation provided by the inverse dynamic model when compared to a measured motor torque. In this regard, the Khalil–Ibrahim model offers the flexibility to include such measurements in the inverse dynamic model but the NOC method does not due to its implementation being wholly in terms of the active joints.

5 Base inertial parameters

The dynamic model of a robot is in terms of the inertial parameters of its rigid bodies. For a rigid body, there are ten inertial parameters, i.e.

$$\boldsymbol{\chi}_i = \left[XX_i\ XY_i\ XZ_i\ YY_i\ YZ_i\ ZZ_i\ MX_i\ MY_i\ MZ_i\ m_i\right]^T. \tag{42}$$

Hence, for a robot with n rigid bodies, the dynamic model is in terms of $10n$ inertial parameters. However, not all of these parameters have a direct impact on the dynamic model. As a result, the number of inertial parameters can be reduced through elimination of these parameters and grouping of other parameters. This reduced set of parameters is known as the base inertial parameters. They are the minimum number of inertial parameters required to compute the dynamic model of a robot [29] and as a result reduce computation cost [23]. Further, knowledge of the base inertial parameters is critical in a dynamic calibration of a robot as they are the only parameters that are identifiable [10, 13, 23].

When the dynamic model of a robot is expressed with respect to the frame origins of the links—not the centre of mass—the model is linear with respect to the inertial parameters of the mechanism [24]. This allows for the inverse dynamic model to be written in a closed linear regressor form, i.e.

$$\boldsymbol{\tau} = \mathbf{D}\boldsymbol{\chi} \tag{43}$$

where $\mathbf{D}$ is the $n \times k$ dynamic regressor of the mechanism in terms of the geometric parameters, joint and task space variables, and $\boldsymbol{\chi}$ is the $k \times 1$ vector of inertial parameters of the parallel mechanism (n is the number of actuators, k is the number of inertial parameters). This regressor form of the inverse dynamic model is utilised in dynamic calibration to solve for the inertial parameters and is also useful in the design of advanced control laws such as a sliding mode controller.

The base inertial parameters can be determined by investigating the linear dependence of the columns of the symbolic regressor matrix or through use of QR decomposition on a numerical regressor [12]. However, as the complexity of the mechanism increases, this becomes a cumbersome task and prone to error. Recursive energy relationships have instead been used to determine the base parameters. This method exploits the fact that the sum of potential and kinetic energy when derived with respect to the frame origin of a rigid body is linear with respect to the inertial parameters [13, 19, 20], i.e.

$$E_j = KE_j + PE_j = \mathbf{e}_j \boldsymbol{\chi}_j \tag{44}$$

where E_j is the total energy of link j, $\mathbf{e}_j$ is a 1×10 vector of the partial derivatives of E_j with respect to the inertial parameters (i.e. an energy function for each inertial parameter) and $\boldsymbol{\chi}_j$ is the 10×1 vector of standard inertial parameters for link j. The expression for the elements of $\mathbf{e}_j$, e_k $(k = 1, \ldots, 10)$ are found in Appendix A. The base parameters are derived using the expressions of e_k as follows [13, 19, 20]:

- If e_k is a constant, then the parameter χ_k has no effect on the dynamic model. Thus, χ_k can be eliminated from $\boldsymbol{\chi}_j$; or
- If e_k can be expressed as a linear combination of $e_{k1}, \ldots, e_{kr}$, i.e. $e_k = \kappa_{k1}e_{k1} + \cdots + \kappa_{kr}e_{kr}$, then χ_k can be grouped with parameters $\chi_{k1}, \ldots, \chi_{kr}$. The grouped parameters take the form $\chi_{Rkm} = \chi_{km} + \kappa_{km}\chi_k$, for $m = 1, \ldots, r$ and replace the associated parameters in $\boldsymbol{\chi}_j$.

Grouping relations for serial robots [13] and those with more complex structures [18] have been derived using the energy relations for prismatic and revolute joints. The rules for serial robots are included in Appendix B for ease of reference, with a thorough explanation provided in [13, 19].

5.1 Base parameters of the serial legs of MEPaM

MEPaM consists of three identical legs which have three links, i.e. each leg has a total of 30 standard inertial parameters. Applying the rules in Appendix B to the serial legs of MEPaM, the number of inertial parameters for each leg is reduced to 7, i.e.

$$\boldsymbol{\chi}_{Ri} = \left[ZZ_{R1i}\ MX_{R1i}\ MY_{1i}\ ZZ_{R2i}\ MX_{R2i}\ MY_{R2i}\ m_{3i}\right]^T. \tag{45}$$

The grouping parameters defined in Eq. (45) are:

$$
\begin{aligned}
ZZ_{R1i} &= ZZ_{1i} + d_{1i}{}^2 m_{2i},\\
MX_{R1i} &= MX_{1i} + d_{1i} m_{2i},\\
ZZ_{R2i} &= ZZ_{2i} + ZZ_{3i} + 2d_{2i} MX_{3i},\\
MX_{R2i} &= MX_{2i} + MX_{3i},\\
MY_{R2i} &= MY_{2i} - MY_{3i}.
\end{aligned}
$$

5.2 Base parameters of the closed loop mechanism

As shown in [20], the recursive energy relations can be used to group parameters of the platform with those of the serial legs. This is achieved by exploiting the velocity condition at the cut joint. For MEPaM, as the origin of $\mathcal{F}_{3i}$ is at the platform vertex B_i, then the velocity of the tip of the serial legs and the platform vertex are the same, i.e.

$$
{}^B\mathbf{v}_{3i} = {}^B\mathbf{v}_P + {}^B\boldsymbol{\omega}_P \times {}^B\boldsymbol{\rho}_i. \tag{46}
$$

Equivalently, the velocity of the common point can be expressed as follows

$$
{}^P\mathbf{v}_{3i} = {}^P\mathbf{v}_P + {}^P\boldsymbol{\omega}_P \times {}^P\boldsymbol{\rho}_i. \tag{47}
$$

Through utilisation of this property and the energy relations, some parameters of the connection link, i.e. link $3i$, can be grouped with parameters of the platform. As is evident from Eq. (45), only the mass of the third link, m_{3i}, has an effect on the dynamics and has not been grouped. Hence, for m_{3i} to be grouped with the parameters of the platform, then the energy function $e_{m3i} = \kappa_{P1} e_{P1} + \cdots + \kappa_{Pr} e_{Pr}$. As shown in Appendix C, the masses m_{3i} can be grouped with the inertial parameters of the platform, forming the following groupings:

$$
\begin{aligned}
XX_{RP} &= XX_P + d_{32}^2 c_2^2 m_{32} + d_{33}^2 c_3^2 m_{33},\\
XY_{RP} &= XY_P + d_{32}^2 s_2 c_2 m_{32} - d_{33}^2 s_3 c_3 m_{33},\\
YY_{RP} &= YY_P + d_{31}^2 m_{31} + d_{32}^2 s_2^2 m_{32} + d_{33}^2 s_3^2 m_{33},\\
ZZ_{RP} &= ZZ_P + d_{31}^2 m_{31} + d_{32}^2 m_{32} + d_{33}^2 m_{33},\\
MX_{RP} &= MX_P + d_{31} m_{31} - d_{32} s_2 m_{32} - d_{33} s_3 m_{33},\\
MY_{RP} &= MY_P + + d_{32} c_2 m_{32} - d_{33} c_3 m_{33},\\
m_{RP} &= m_P + m_{31} + m_{32} + m_{33}
\end{aligned}
$$

with the parameters XZ_P, YZ_P and MZ_P being unchanged.

By grouping the m_{3i} parameters with the parameters of the platform, the parameter vector $\boldsymbol{\chi}$ is independent of the inertial parameters of the third links of the serial chains which correspond to the passive joints of MEPaM. Hence, the dynamic model of MEPaM is independent of these parameters and thus the passive joint rates. This is significant as it means that there is no need to calculate these rates via Eqs. (16) and (17). Further, the model has been reduced from 100 inertial parameters to 28 inertial parameters, reducing the number of computations required. When using the base inertial parameters, the wrenches (written in terms of the base parameters) and twists of the links $3i$ can be omitted in the NOC method.

Table 2 Inertial Parameters of MEPaM ($i = 1, 2, 3$)

j	${}^j\mathbf{I}_j \times 10^{-6}$ [kg m^2]	${}^j\mathbf{ms}_j$ [kg m]	m_j [kg]
$1i$	$\begin{bmatrix} 2.851 & 0 & -0.7160 \\ 0 & 196.5 & 0 \\ -0.7160 & 0 & 199.0 \end{bmatrix}$	$\begin{bmatrix} 0.0021 \\ 0 \\ -5.913 \times 10^{-6} \end{bmatrix}$	0.0415
$2i$	$\begin{bmatrix} 25.28 & 2.961 & 15.32 \\ 2.961 & 266.6 & -0.0150 \\ 15.32 & -0.0150 & 243.6 \end{bmatrix}$	$\begin{bmatrix} 0.0023 \\ 3.906 \times 10^{-5} \\ -4.576 \times 10^{-4} \end{bmatrix}$	0.0544
$3i$	$\begin{bmatrix} 524.9 & 0 & 0 \\ 0 & 524.9 & 0 \\ 0 & 0 & 0.1970 \end{bmatrix}$	$\begin{bmatrix} 0 \\ 0 \\ -3.94 \times 10^{-3} \end{bmatrix}$	0.0394
P	$\begin{bmatrix} 34.16 & -0.0500 & -0.0070 \\ -0.0500 & 34.10 & 0.0160 \\ -0.0070 & 0.0160 & 63.13 \end{bmatrix}$	$\begin{bmatrix} 3.723 \\ -6.101 \\ 33.97 \end{bmatrix} \times 10^{-6}$	0.0809

This reduces the maximum dimension of the matrices from 60 to 42. For the Khalil–Ibrahim method, Eq. (40) is altered to

$$\boldsymbol{\lambda} = \mathbf{h}^a + {}^B\mathbf{J}_M^{T\,B}\mathbf{w}_P. \tag{48}$$

6 Simulation

Simulations were conducted to verify that the NOC and Khalil–Ibrahim methods are equivalent. To do so, a trajectory profile was simulated and the torque profile computed using the two methods. These profiles were compared with a Sim Mechanics model to verify that they produce the correct output. The legs of MEPaM were modelled as RRCU mechanisms in Sim Mechanics to validate the assumption used in the modelling procedure, i.e. that the legs can be modelled as RRPS mechanisms. Further, a different trajectory profile was used to verify if the inverse dynamics models computed using the base inertial parameter set produced the correct output, with comparison made with the Sim Mechanics model which used the full inertial parameter set.

6.1 Geometric and inertial parameters

The architecture of MEPaM under study has the three legs attached to frames that form an equilateral triangle, i.e. $r_i = 0.167$ m, $\gamma_1 = \pi/2$, $\gamma_2 = 7\pi/6$ and $\gamma_3 = 11\pi/6$ in Table 1. The origin of Lever Arm A in $\mathcal{F}_{1i}$ is given by $w_{xi} = 0$ m and $w_{zi} = 0.11$ m. Further, it is assumed that the lengths of Lever Arm A and Lever Arm B are equivalent for the three legs, i.e. $d_{1i} = 0.137$ m and $d_{2i} = 0.1375$ m. As the legs have the same geometric parameters, the inertial parameters are also the same. The platform is assumed to be an equilateral triangle with $d_{3i} = 0.052$ m and $\psi_2 = \psi_3 = \pi/6$. The location of the three platform vertices in $\mathcal{F}_P$ are given by Eq. (5). The inertial parameters of MEPaM are given in Table 2.

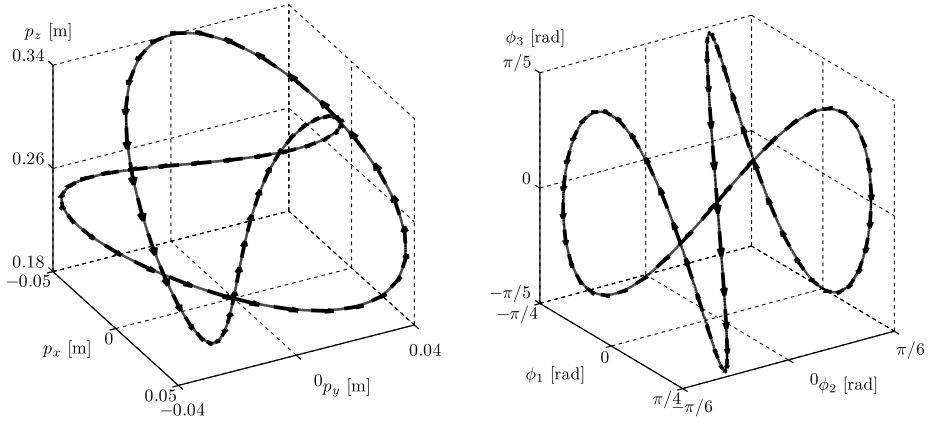

(a) Position (b) Orientation

Fig. 5 Trajectory for validation of inverse dynamic models using complete inertial parameter set ($n_x = 6$, $n_y = 4$, $n_z = 4$, $n_1 = 4$, $n_2 = 2$, $n_3 = 6$, $T_d = 10$)

6.2 Trajectory and torque profiles

The workspace trajectory for the simulations was given by

$$p_x = 0.05 \sin\left(\frac{n_x \pi t}{T_d}\right), \quad p_y = 0.04 \sin\left(\frac{n_y \pi t}{T_d}\right), \quad p_z = 0.26 + 0.07 \sin\left(\frac{n_z \pi t}{T_d} + \frac{3\pi}{2}\right),$$
$$\phi_1 = \frac{\pi}{4} \sin\left(\frac{n_1 \pi t}{T_d}\right), \quad \phi_2 = \frac{\pi}{6} \sin\left(\frac{n_2 \pi t}{T_d}\right), \quad \phi_3 = \frac{\pi}{5} \sin\left(\frac{n_3 \pi t}{T_d}\right)$$

where ϕ_1, ϕ_2 and ϕ_3 are ZYX Euler angles used to describe the orientation of the platform, n_x, n_y, n_z, n_1, n_2 and n_3 are integers that control the frequency of the trajectory, and T_d is the duration of the trajectory.

The trajectory used to verify the inverse dynamic models when calculated using the complete inertial parameter set is shown in Fig. 5. The required joint space trajectory was calculated using the inverse geometric model, with the result used to calculate the required torques through the inverse dynamics. The computed torques using the two models and Sim Mechanics are shown in Fig. 6. A different trajectory was used to verify the inverse dynamic models in terms of the base parameters, with the computed torques shown in Fig. 7. Note that the torque profile produce by Sim Mechanics used the complete inertial parameter set.

From Figs. 6 and 7, it is evident that the NOC and Khalil–Ibrahim methods produce the same computed torque outputs when using the complete and base inertial parameter sets. Further, the simulations show that the torque profiles are the same as the Sim Mechanics model, indicating correctness of the models and validating the assumption made in modelling that the legs can be treated as RRPS mechanisms. Using the complete inertial parameter set, the Khalil–Ibrahim method involved 546 multiplications and 357 additions whilst the NOC method involved 80 172 multiplications and 79 194 additions. Using the base inertial parameters, the Khalil–Ibrahim method was reduced to 237 multiplications and 162 additions whilst the NOC method was reduced to 40 266 multiplications and 39 558 additions, i.e. it is advantageous to use the base inertial parameters when considering computation cost. The vast amount of operations in the NOC method is to be expected as it

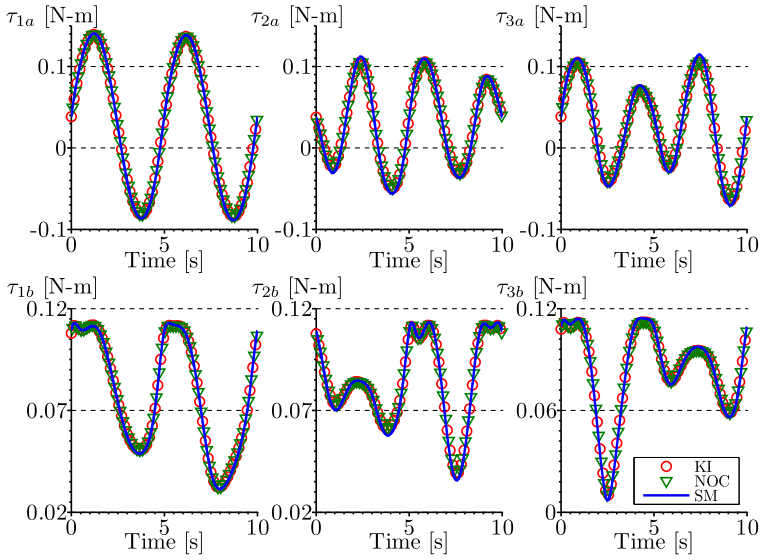

Fig. 6 Computed torques using complete inertial parameter set (KI—Khalil–Ibrahim, NOC—Natural Orthogonal Complement, SM—Sim Mechanics)

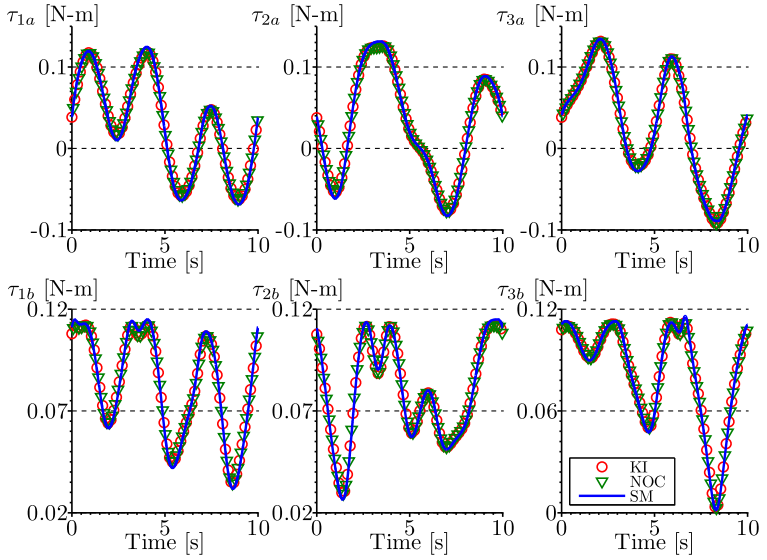

Fig. 7 Computed torques using base inertial parameter set ($n_x = 4$, $n_y = 6$, $n_z = 6$, $n_1 = 2$, $n_2 = 6$, $n_3 = 4$, $T_d = 10$)

involves large matrices—the largest being 60×60—while the largest matrix involved in the Khalil–Ibrahim method has dimension 6×6. Hence, the Khalil–Ibrahim method is more efficient, benefiting from the use of the closed form inverse dynamic models of the serial legs.

7 Conclusion

The inverse dynamic model of a novel six-degree-of-freedom three-legged parallel mechanism was derived using the NOC and Khalil–Ibrahim methods. These methods yielded closed form expressions which can be expressed wholly in terms of the active joint variables. Simulations and comparisons with a Sim Mechanics model showed these models to be equivalent and correct, with the Khalil–Ibrahim method being more computationally efficient. Further, the models were reduced to 28 base inertial parameters—completely independent of the inertial parameters related to the passive joints—which reduced the computation cost of both methods by approximately 50 %.

Appendix A: Recursive energy relations

Letting the transformation matrix ${}^{B}\mathbf{T}_j = \left[\begin{smallmatrix} \mathbf{i} & \mathbf{j} & \mathbf{k} & {}^{B}\mathbf{p}_j \\ 0 & 0 & 0 & 1 \end{smallmatrix}\right]$ with $\mathbf{i}$, $\mathbf{j}$ and $\mathbf{k}$ being 3×1 vectors which describe the orientation of link j with respect to the base frame, the angular velocity of link j be $\boldsymbol{\omega}_j = [\omega_{xj}\ \omega_{yj}\ \omega_{zj}]^T$ and the linear velocity of link j be $\mathbf{v}_j = [v_{xj}\ v_{yj}\ v_{zj}]^T$, the recursive energy relations associated with the link's inertial parameter vector $\boldsymbol{\chi}_j$ are [19, 20]

$$
\begin{aligned}
e_{XX_j} &= \frac{1}{2}\omega_{xj}^2, & e_{XY_j} &= \omega_{xj}\omega_{yj}, \\
e_{XZ_j} &= \omega_{xj}\omega_{zj}, & e_{YY_j} &= \frac{1}{2}\omega_{yj}^2, \\
e_{YZ_j} &= \omega_{yj}\omega_{zj}, & e_{ZZ_j} &= \frac{1}{2}\omega_{zj}^2, \\
e_{MX_j} &= \omega_{xj}v_{yj} - \omega_{yj}v_{zj} - {}^{B}\mathbf{g}^T\mathbf{i}, & e_{MY_j} &= \omega_{xj}v_{zj} - \omega_{zj}v_{xj} - {}^{B}\mathbf{g}^T\mathbf{j}, \\
e_{MZ_j} &= \omega_{zj}v_{xj} - \omega_{xj}v_{zj} - {}^{B}\mathbf{g}^T\mathbf{k}, & e_{m_j} &= \frac{1}{2}\mathbf{v}_j^T\mathbf{v}_j - {}^{B}\mathbf{g}^T{}^{B}\mathbf{p}_j.
\end{aligned}
\tag{49}
$$

Appendix B: Grouping relations for serial legs

A complete derivation and overview of the grouping relations for serial and tree robots can be found in [13, 18, 19]. The rules and expressions used to determine the base inertial parameters of the serial legs of MEPaM are considered below. Using the rules developed in [13, 18, 19], where possible, the parameters of link $3i$ were grouped with the parameters of link $2i$ which were subsequently grouped with the parameters of link $1i$. With reference to Table 1, $\gamma_j = 0$ and $b_j = 0$ for $j = 2$ and 3, hence the rules which pertain to serial robots suffice. These are (in terms of the Khalil–Kleinfinger parameters):

– If joint j is revolute, the parameters YY_j, MZ_j and m_j can be grouped with the parameters of link j and link $j-1$. The resulting parameters are:

$$
\begin{aligned}
XX_{Rj} &= XX_j - YY_j, \\
XX_{Rj-1} &= XX_{j-1} + YY_j + 2d_jMZ_j + {d_j}^2m_j, \\
XY_{Rj-1} &= XY_{j-1} + a_js_{\alpha_j}MZ_j + a_jd_js_{\alpha_j}m_j, \\
XZ_{Rj-1} &= XZ_{j-1} - a_jc_{\alpha_j}MZ_j - a_jd_jc_{\alpha_j}m_j,
\end{aligned}
$$

$$
\begin{aligned}
YY_{Rj-1} &= YY_{j-1} + c_{\alpha_j}^2 YY_j + 2d_j c_{\alpha_j}^2 MZ_j + \left(a_j^2 + d_j^2 {c_{\alpha_j}}^2\right) m_j,\\
YZ_{Rj-1} &= YZ_{j-1} + c_{\alpha_j} s_{\alpha_j} YY_j + 2d_j c_{\alpha_j} s_{\alpha_j} MZ_j + {d_j}^2 c_{\alpha_j} s_{\alpha_j} m_j,\\
ZZ_{Rj-1} &= ZZ_{j-1} + s_{\alpha_j}^2 YY_j + 2d_j s_{\alpha_j}^2 MZ_j + \left(a_j^2 + d_j^2 {s_{\alpha_j}}^2\right) m_j,\\
MX_{Rj-1} &= MX_{j-1} + a_j M_j,\\
MY_{Rj-1} &= MY_{j-1} - s_{\alpha_j} MZ_j - d_j s_{\alpha_j} m_j,\\
MZ_{Rj-1} &= MZ_{j-1} + c_{\alpha_j} MZ_j + d_j c_{\alpha_j} m_j.\\
m_{Rj-1} &= m_{j-1} + m_j.
\end{aligned}
$$

– If joint j is prismatic, the parameters of the inertia tensor of link j (XX_j, XY_j, XZ_j, YY_j, YZ_j, ZZ_j) can be grouped with those of link $j-1$. The resulting parameters are:

$$
\begin{aligned}
XX_{Rj-1} &= XX_{j-1} + {c_{\theta_j}}^2 XX_j - 2c_{\theta_j} s_{\theta_j} XY_j + {s_{\theta_j}}^2 YY_j,\\
XY_{Rj-1} &= XY_{j-1} + c_{\theta_j} s_{\theta_j} c_{\alpha_j} XX_j + \left(c_{\theta_j}^2 - s_{\theta_j}^2\right) c_{\alpha_j} XY_j - c_{\theta_j} s_{\alpha_j} XZ_j\\
&\quad - c_{\theta_j} s_{\theta_j} c_{\alpha_j} YY_j + s_{\theta_j} s_{\alpha_j} YZ_j,\\
XZ_{Rj-1} &= XZ_{j-1} + c_{\theta_j} s_{\theta_j} s_{\alpha_j} XX_j + \left(c_{\theta_j}^2 - s_{\theta_j}^2\right) s_{\alpha_j} XY_j + c_{\theta_j} c_{\alpha_j} XZ_j\\
&\quad - c_{\theta_j} s_{\theta_j} s_{\alpha_j} YY_j - s_{\theta_j} c_{\alpha_j} YZ_j,\\
YY_{Rj-1} &= YY_{j-1} + s_{\theta_j}^2 c_{\alpha_j}^2 XX_j + 2c_{\theta_j} s_{\theta_j} c_{\alpha_j}^2 XY_j - 2s_{\theta_j} c_{\alpha_j} s_{\alpha_j} XZ_j + c_{\theta_j}^2 c_{\alpha_j}^2 YY_j\\
&\quad - 2c_{\theta_j} c_{\alpha_j} s_{\alpha_j} YZ_j + s_{\alpha_j}^2 ZZ_j,\\
YZ_{Rj-1} &= YZ_{j-1} + s_{\theta_j}^2 c_{\alpha_j} s_{\alpha_j} XX_j + 2c_{\theta_j} s_{\theta_j} c_{\alpha_j} s_{\alpha_j} XY_j + s_{\theta_j} \left(c_{\alpha_j}^2 - s_{\alpha_j}^2\right) XZ_j\\
&\quad + c_{\theta_j}^2 c_{\alpha_j} s_{\alpha_j} YY_j + 2c_{\theta_j} \left(c_{\alpha_j}^2 - s_{\alpha_j}^2\right) YZ_j - c_{\alpha_j} s_{\alpha_j} ZZ_j,\\
ZZ_{Rj-1} &= ZZ_{j-1} + s_{\theta_j}^2 s_{\alpha_j}^2 XX_j + 2c_{\theta_j} s_{\theta_j} s_{\alpha_j}^2 XY_j + 2s_{\theta_j} c_{\alpha_j} s_{\alpha_j} XZ_j + c_{\theta_j}^2 s_{\alpha_j}^2 YY_j\\
&\quad + 2c_{\theta_j} c_{\alpha_j} s_{\alpha_j} YZ_j + c_{\alpha_j}^2 ZZ_j.
\end{aligned}
$$

– If the axis of the prismatic joint j is parallel to the nearest revolute joint axis i (i is not necessarily $j-1$), then MZ_j has no effect on the dynamic model and the parameters MX_j and MY_j can be grouped as follows:

$$
\begin{aligned}
MX_{Rj-1} &= MX_{j-1} + c_{\theta_j} MX_j - s_{\theta_j} MY_j,\\
MY_{Rj-1} &= MY_{j-1} + s_{\theta_j} c_{\alpha_j} MX_j + c_{\theta_j} c_{\alpha_j} MY_j,\\
MZ_{Rj-1} &= MZ_{j-1} + s_{\theta_j} s_{\alpha_j} MX_j + c_{\theta_j} s_{\alpha_j} MY_j,\\
ZZ_{Ri} &= ZZ_i + 2a_j c_{\theta_j} MX_j - 2a_j s_{\theta_j} MY_j.
\end{aligned}
$$

– If joint j is revolute and articulated on the base, the parameters XX_j, XY_j, XZ_j, YY_j, YZ_j, MZ_j and m_j have no effect on the dynamic model and can be eliminated.

Appendix C: Grouping leg parameters with platform

For the parameters m_{3i} to be grouped with the parameters of the platform, the energy function $e_{m_{3i}}$ needs to be in a form that is a linear combination of the platform energy functions, i.e.

$$e_{m_{3i}} = \kappa_1 e_{XX_P} + \kappa_2 e_{XY_P} + \cdots + \kappa_{10} e_{m_P}. \tag{50}$$

This is possible by use of the velocity of the connection point of the legs to the platform, i.e.

$${}^P\mathbf{v}_{3i} = {}^P\mathbf{v}_P + {}^P\boldsymbol{\omega}_P \times {}^P\boldsymbol{\rho}_i \tag{51}$$

where ${}^P\mathbf{v}_P = [{}^P v_{xP}\ {}^P v_{yP}\ {}^P v_{zP}]^T$, ${}^P\boldsymbol{\omega}_P = [{}^P\omega_{xP}\ {}^P\omega_{yP}\ {}^P\omega_{zP}]^T$ and ${}^P\boldsymbol{\rho}_i = [{}^P b_{xi}\ {}^P b_{yi}\ {}^P b_{zi}]^T$.

Let the transformation of the platform frame to the base frame be

$${}^B\mathbf{T}_P = \begin{bmatrix} \mathbf{i}\ \mathbf{j}\ \mathbf{k}\ {}^B\mathbf{p}_P \\ 0\,0\,0\ \ 1 \end{bmatrix} \tag{52}$$

where $\mathbf{i}$, $\mathbf{j}$ and $\mathbf{k}$ are 3×1 vectors which describe the orientation of the platform with respect to the base frame and ${}^B\mathbf{p}_P$ is the translation between the origin of the two frames. Then the co-ordinates of the connection points in the base frame are

$$\begin{aligned} {}^B\mathbf{b}_i &= \begin{bmatrix} \mathbf{i}\ \mathbf{j}\ \mathbf{k}\ {}^B\mathbf{p}_P \\ 0\,0\,0\ \ 1 \end{bmatrix} \begin{bmatrix} {}^P\mathbf{b}_i \\ 1 \end{bmatrix} \\ &= {}^B\mathbf{p}_P + {}^P b_{xi}\mathbf{i} + {}^P b_{yi}\mathbf{j} + {}^P b_{iz}\mathbf{k}. \end{aligned} \tag{53}$$

Therefore, the energy function for the masses m_{3i} can be determined using Eq. (49) for e_{m_j}, Eq. (51) for the velocity of link $3i$ and Eq. (53) for the connection point expressed in $\mathcal{F}_B$, i.e.

$$\begin{aligned} e_{m_{3i}} &= \frac{1}{2}{}^P\mathbf{v}_{3i}^T\,{}^P\mathbf{v}_{3i} - {}^B\mathbf{g}^T\,{}^B\mathbf{b}_i \\ &= \frac{1}{2}\left({}^P b_{yi}{}^2 + {}^P b_{zi}{}^2\right){}^P\omega_{xP}{}^2 - {}^P b_{xi}\,{}^P b_{yi}\,{}^P\omega_{xP}\,{}^P\omega_{yP} - {}^P b_{xi}\,{}^P b_{zi}\,{}^P\omega_{xP}\,{}^P\omega_{zP} \\ &\quad + \frac{1}{2}\left({}^P b_{xi}{}^2 + {}^P b_{zi}{}^2\right){}^P\omega_{yP}{}^2 - {}^P b_{yi}\,{}^P b_{zi}\,{}^P\omega_{yP}\,{}^P\omega_{zP} + \frac{1}{2}\left({}^P b_{xi}{}^2 + {}^P b_{yi}{}^2\right){}^P\omega_{zP}{}^2 \\ &\quad + {}^P b_{xi}\left({}^P\omega_{zP}\,{}^P v_{yP} - {}^P\omega_{yP}\,{}^P v_{zP} - {}^B\mathbf{g}^T\mathbf{i}\right) + {}^P b_{yi}\left({}^P\omega_{xP}\,{}^P v_{zP} - {}^P\omega_{zP}\,{}^P v_{xP} - {}^B\mathbf{g}^T\mathbf{j}\right) \\ &\quad + {}^P b_{zi}\left({}^P\omega_{yP}\,{}^P v_{xP} - {}^P\omega_{xP}\,{}^P v_{yP} - {}^B\mathbf{g}^T\mathbf{k}\right) + \frac{1}{2}{}^P\mathbf{v}_P^T\,{}^P\mathbf{v}_P - {}^B\mathbf{g}^T\,{}^B\mathbf{p}_P. \end{aligned} \tag{54}$$

With aid of Eq. (49), Eq. (54) is rearranged to

$$\begin{aligned} e_{m_{3i}} &= \left({}^P b_{yi}{}^2 + {}^P b_{zi}{}^2\right)e_{XX_P} - {}^P b_{xi}\,{}^P b_{yi}\,e_{XY_P} - {}^P b_{xi}\,{}^P b_{zi}\,e_{XZ_P} + \left({}^P b_{xi}{}^2 + {}^P b_{zi}{}^2\right)e_{YY_P} \\ &\quad - {}^P b_{yi}\,{}^P b_{zi}\,e_{YZ_P} + \left({}^P b_{xi}{}^2 + {}^P b_{yi}{}^2\right)e_{ZZ_P} + {}^P b_{xi}\,e_{MX_P} \\ &\quad + {}^P b_{yi}\,e_{MY_P} + {}^P b_{zi}\,e_{MZ_P} + e_{m_P}. \end{aligned} \tag{55}$$

As a result of Eq. (55), it is possible to group the m_{3i} parameters with the inertial parameters of the platform. Due to the assignment of the platform frame, $\mathcal{F}_P$, the co-ordinates of the

platform vertices in $\mathcal{F}_P$ are:

$$ {}^P\mathbf{b}_1 = \begin{bmatrix} d_{31} \\ 0 \\ 0 \end{bmatrix}, \qquad {}^P\mathbf{b}_2 = \begin{bmatrix} -d_{32}s_2 \\ d_{32}c_2 \\ 0 \end{bmatrix}, \qquad {}^P\mathbf{b}_3 = \begin{bmatrix} -d_{33}s_3 \\ -d_{33}c_3 \\ 0 \end{bmatrix}. $$

Hence, the grouping relations are

$$ XX_{RP} = XX_P + \sum_{i=1}^{3} \left({}^P b_{yi}{}^2 + {}^P b_{zi}{}^2 \right) m_{3i} = XX_P + d_{32}^2 c_2^2 m_{32} + d_{33}^2 c_3^2 m_{33}, $$

$$ XY_{RP} = XY_P - \sum_{i=1}^{3} {}^P b_{xi}\, {}^P b_{yi} m_{3i} = XY_P + d_{32}^2 s_2 c_2 m_{32} - d_{33}^2 s_3 c_3 m_{33}, $$

$$ XZ_{RP} = XZ_P - \sum_{i=1}^{3} {}^P b_{xi}\, {}^P b_{zi} m_{3i} = XZ_P, $$

$$ YY_{RP} = YY_P + \sum_{i=1}^{3} \left({}^P b_{xi}{}^2 + {}^P b_{zi}{}^2 \right) m_{3i} = YY_P + d_{31}^2 m_{31} + d_{32}^2 s_2^2 m_{32} + d_{33}^2 s_3^2 m_{33}, $$

$$ YZ_{RP} = YZ_P - \sum_{i=1}^{3} {}^P b_{yi}\, {}^P b_{zi} m_{3i} = YZ_P, $$

$$ ZZ_{RP} = ZZ_P + \sum_{i=1}^{3} \left({}^P b_{xi}{}^2 + {}^P b_{yi}{}^2 \right) m_{3i} = ZZ_P + d_{31}^2 m_{31} + d_{32}^2 m_{32} + d_{33}^2 m_{33}, $$

$$ MX_{RP} = MX_P + \sum_{i=1}^{3} {}^P b_{xi} m_{3i} = MX_P + d_{31} m_{31} - d_{32} s_2 m_{32} - d_{33} s_3 m_{33}, $$

$$ MY_{RP} = MY_P + \sum_{i=1}^{3} {}^P b_{yi} m_{3i} = MY_P + d_{32} c_2 m_{32} - d_{33} c_3 m_{33}, $$

$$ MZ_{RP} = MZ_P + \sum_{i=1}^{3} {}^P b_{zi} m_{3i} = MZ_P, $$

$$ m_{RP} = m_P + \sum_{i=1}^{3} m_{3i} = m_P + m_{31} + m_{32} + m_{33}. $$

References

1. Akbarzadeh, A., Enferadi, J., Sharifnia, M.: Dynamics analysis of a 3-RRP spherical parallel manipulator using the natural orthogonal complement. Multibody Syst. Dyn. **29**(4), 361–380 (2013)
2. Angeles, J.: Fundamentals of Robotic Mechanical Systems: Theory, Methods and Algorithms, 3rd edn. Springer, Berlin (2007)

3. Angeles, J., Lee, S.: The formulation of dynamical equations of holonomic mechanical systems using a natural orthogonal complement. J. Appl. Mech. **55**(1), 243–244 (1988)
4. Angeles, J., Ma, O.: Dynamic simulation of n-axis serial robotic manipulators using a natural orthogonal complement. Int. J. Robot. Res. **7**(5), 32–47 (1988)
5. Chen, C., Gayral, T., Caro, S., Chablat, D., Moroz, G., Abeywardena, S.: A six degree of freedom epicyclic-parallel manipulator. J. Mech. Robot. **4**(4), 041011 (2012)
6. Cleary, K., Brooks, T.: Kinematic analysis of a novel 6-dof parallel manipulator. In: IEEE International Conference on Robotics and Automation, pp. 708–713 (1993)
7. Craig, J.: Introduction to Robotics: Mechanics and Control, 3rd edn. Prentice Hall, New York (2005)
8. Dasgupta, B., Mruthyunjaya, T.: A Newton–Euler formulation for the inverse dynamics of the Stewart platform manipulator. Mech. Mach. Theory **33**(8), 1135–1152 (1998)
9. Enferadi, J., Akbarzadeh, A.: Inverse dynamics analysis of a general spherical star-triangle parallel manipulator using principle of virtual work. Nonlinear Dyn. (2010)
10. Farhat, N., Mata, V., Page, A., Valero, F.: Identification of dynamic parameters of a 3-dof RPS parallel manipulator. Mech. Mach. Theory **43**(1), 1–17 (2008)
11. Fattah, A., Kasaei, G.: Kinematics and dynamics of a parallel manipulator with a new architecture. Robotica **18**, 535–543 (2000)
12. Gautier, M.: Numerical calculation of the base inertial parameters of robots. J. Robot. Syst. **8**(4), 485–506 (1991)
13. Gautier, M., Khalil, W.: Direct Calculation of minimum set of inertial parameters of serial robots. IEEE Trans. Robot. Autom. **6**(3), 368–373 (1990)
14. Geng, Z., Haynes, L.S., Lee, J.D., Carroll, R.L.: On the dynamic model and kinematic analysis of a class of Stewart platforms. Robot. Auton. Syst. **9**(4), 237–254 (1992)
15. Gosselin, C.: Parallel computational algorithms for the kinematics and dynamics of planar and spatial parallel manipulators. J. Dyn. Syst. Meas. Control **118**(1), 22–28 (1996)
16. Guegan, S., Khalil, W.: Dynamic modeling of the Orthoglide. In: Lenarčič, J., Thomas, F. (eds.) Advances in Robot Kinematics, pp. 387–396. Springer, Netherlands (2002)
17. Ibrahim, O., Khalil, W.: Kinematic and dynamic modeling of the 3-rps parallel manipulator. In: Proc. 12th IFToMM World Congress, vol. 19, pp. 95–100 (2007)
18. Khalil, W., Bennis, F.: Symbolic calculation of the base inertial parameters of closed-loop robots. Int. J. Robot. Res. **14**(2), 112–128 (1995)
19. Khalil, W., Dombre, E.: Modeling, Identification and Control of Robots. Butterworth-Heinemann, Oxford (2004)
20. Khalil, W., Guegan, S.: Inverse and direct dynamic modelling of Gough–Stewart robots. IEEE Trans. Robot. Autom. **20**(4), 754–762 (2004)
21. Khalil, W., Ibrahim, O.: General solution for the dynamic modelling of parallel robots. J. Intell. Robot. Syst. **49**(1), 19–37 (2007)
22. Khalil, W., Kleinfinger, J.: A new geometric notation for open and closed-loop robots. In: Proceedings of IEEE International Conference on Robotics and Automation, vol. 3, pp. 1174–1179 (1986)
23. Khalil, W., Kleinfinger, J.F.: Minimum operations and minimum parameters of the dynamic models of tree structure robots. IEEE J. Robot. Autom. **3**(6), 517–526 (1987)
24. Khosla, P., Kanade, T.: Parameter identification of robot dynamics. In: 24th IEEE Conference on Decision and Control, vol. 24, pp. 1754–1760 (1985). 1985
25. Lebret, G., Liu, K., Lewis, F.L.: Dynamic analysis and control of a Stewart platform manipulator. J. Robot. Syst. **10**(5), 629–655 (1993)
26. Lee, S.U., Kim, S.: Analysis and optimal design of a new 6-dof parallel type haptic device. In: IEEE/RSJ International Conference on Intelligent Robots and Systems, pp. 460–465 (2006)
27. Liu, M.J., Li, C.X., Li, C.N.: Dynamics analysis of the Gough–Stewart platform manipulator. IEEE Trans. Robot. Autom. **16**(1), 94–98 (2000)
28. Ma, O.: Mechanical analysis of parallel manipulators with simulation, design, and control applications. PhD thesis, McGill University (1991)
29. Mayeda, H., Yoshida, K., Osuka, K.: Base parameters of manipulator dynamic models. IEEE Trans. Robot. Autom. **6**(3), 312–321 (1990)
30. Monsarrat, B., Gosselin, C.: Workspace analysis and optimal design of a 3-leg 6-dof parallel platform mechanism. IEEE Trans. Robot. Autom. **19**(6), 954–966 (2003)
31. Rao, A., Saha, S., Rao, P.: Dynamics modelling of hexaslides using the decoupled natural orthogonal complement matrices. Multibody Syst. Dyn. **15**(2), 159–180 (2006)
32. Tsai, L.: Solving the inverse dynamics of a Stewart–Gough manipulator by the principle of virtual work. J. Mech. Des. **122**, 3–9 (2000)

33. Wang, J., Gosselin, C.: A new approach for the dynamic analysis of parallel manipulators. Multibody Syst. Dyn. **2**(3), 317–334 (1998)
34. Xi, F., Sinatra, F.: Inverse dynamics of hexapods using the natural orthogonal complement method. J. Manuf. Syst. **21**(2), 73–82 (2002)
35. Zanganeh, K.E., Sinatra, R., Angeles, J.: Kinematics and dynamics of a six-degree-of-freedom parallel manipulator with revolute legs. Robotica **15**, 385–394 (1997)